ELSEVIER

Nuclear Instruments and Methods in Physics Research B 183 (2001) 16–24

NIM B
Beam Interactions with Materials & Atoms

www.elsevier.com/locate/nimb

Limitations to depth resolution in ion scattering experiments

W.H. Schulte [a,*], B.W. Busch [a], E. Garfunkel [a], T. Gustafsson [a], G. Schiwietz [b], P.L. Grande [c]

[a] *Departments of Physics and Chemistry and Laboratory for Surface Modification, Rutgers University, 136 Frelinghuysen Rd., Piscataway, NJ 08854-8019, USA*

[b] *Bereich F, Hahn-Meitner-Institut Berlin, Glienicker Str. 100, D-14109 Berlin, Germany*

[c] *Instituto de Física da Universidade Federal do Rio Grande do Sul, Caixa Postal 15051, 91501-970 Porto Alegre, RS, Brazil*

Received 26 October 2000; received in revised form 19 December 2000

Abstract

The energy spectra of scattered ions in Rutherford backscattering and elastic recoil scattering experiments are commonly described using stopping power and straggling data. These, in turn, are based on statistical approximations and thus neglect the characteristics of individual ion–atom collisions. This simplified analysis is not justified when considering experiments with high-energy resolution. We have performed theoretical and experimental studies to understand the shape of high-energy resolution ion scattering spectra. The impact parameter dependent energy loss in single ion–atom collisions has been calculated using the semi-classical approximation (SCA). We show that limitations for extracting monolayer depth resolution become obvious from this non-statistical approach. Experiments were performed using a medium energy ion scattering (MEIS) system. For the case of 100 keV protons scattered on sulfur atoms, good agreement between the theoretical description and experimental data was found. The influence of thermal vibrations of the sample atoms on the backscattering spectra is discussed.

Keywords: Stopping power; Energy loss; Protons; Ion beams; Ion scattering

1. Introduction

Different ion scattering techniques, such as elastic recoil detection (ERD) and medium energy ion scattering (MEIS) have proven to be powerful tools for determining the composition of thin films. Complementary to the technological requirement to understand the growth processes of ultra-thin films, an increasing demand for quantitative analytical techniques to characterize these structures has become obvious during the last few years. [1] The strong technical efforts for achieving monolayer resolution by using high-resolution time-of-flight, magnetic and electrostatic spec-

* Corresponding author.
E-mail address: hartmut@physics.rutgers.edu (W.H. Schulte).

[1] See other contributions to this topical issue.

0168-583X/01/$ - see front matter
PII: S0168-583X(01)00313-5

trometers for particle detection, as well as by applying grazing angle geometry, however, have not been accompanied by substantial improvements of analyzing the energy spectra.

The aim of the present paper is not to review the effects that may influence the shape of high-resolution scattering spectra in a comprehensive manner. Instead we want to present some examples, showing that a more detailed analysis of high-resolution spectra compared to standard Rutherford backscattering spectrometry (RBS), i.e. using silicon surface barrier detectors for measuring the energy of backscattered He projectiles, has to be applied. To contribute to a more thorough understanding of the shape of single collision energy loss spectra we performed theoretical studies based on the semi-classical approximation (SCA) as well as MEIS experiments on sub-monolayer surface coverages. In order to reduce additional complications due to charge exchange processes, we will here concentrate on fast light projectiles [1].

Work on narrow nuclear resonances has clearly demonstrated not only the influence of individual electron excitation processes on the corresponding yield curves, but also the influence of Doppler broadening [2–9]. The underlying interaction of projectiles with matter is identical for scattering and nuclear resonance work in terms of slowing down the projectiles before the scattering process or the nuclear resonance reaction, therefore we present also examples from the latter work.

2. Basic considerations

Projectiles in an ion scattering experiment are deflected due to Coulomb interaction with the sample nuclei. Scattering events from surface layers can be considered as a single collision at a very small impact parameter. Scattering from deeper layers may involve consecutive energy losses (for light projectiles predominantly due to electron excitation and ionization of sample atoms) before the small impact parameter collision occurs. Due to the use of silicon surface barrier detectors as energy analyzer, standard ion scattering experiments offer only limited depth resolution (in the range of 2–10 nm), not allowing identification of single energy loss processes. Significantly improved depth resolution can be achieved with magnetic or electrostatic spectrometers or time-of-flight techniques. In some cases a resolution approaching one atomic monolayer has been reported. [1] For these cases, clearly, an atomistic description of the energy losses should be considered.

Scattering from thin surface layers can provide information on the experimental energy resolution. For most practical cases it can be assumed that the energy spectrum of a sub-monolayer surface layer is represented by a sharp peak due to elastic scattering processes, convoluted with the experimental resolution ΔE.

$$\Delta E = (\Delta E_{\mathrm{D}}^2 + \Delta E_{\mathrm{S}}^2 + \Delta E_{\mathrm{p}}^2)^{1/2}. \quad (1)$$

ΔE is described by contributions from the energy spread of the projectiles ΔE_{p}, the energy resolution of the spectrometer ΔE_{S} and the effect of thermal Doppler broadening due to the motion of the sample atoms ΔE_{D}. Frequently these contributions can be assumed to be Gaussian. [2] With excellent energy resolution, however, this simplified description is no longer valid. Instead details of the single collision become visible.

It should be noted that monolayer resolution of MEIS depth profiles has been observed without a detailed discussion of the energy loss processes. High-precision channeling and blocking studies of crystalline samples allow not only the precise determination of the lattice structure, vibrational amplitudes, and defects, but they allow in specific cases layer resolved depth profiling of elements contained in the outer layers of crystalline structures [10,11].

In high-resolution MEIS experiments various attempts have been made to fit the energy spectra using impact parameter dependent models for the energy loss. For example, Alkemade et al. [13,14] used a Monte Carlo simulation based on the model

[2] It should, however, be noted that charge exchange processes may lead to a non-Gaussian shape of the ion beam energy spread of Tandem accelerators and that significant non-statistical fluctuations of accelerating voltages may also lead to non-Gaussian energy distributions.

developed by Frenken et al. [12] to describe He and H scattering spectra from crystalline samples.

Narrow nuclear resonance reactions are present in proton induced reactions on various light isotopes. These resonances have been used for basic studies of energy loss processes and for depth profiling applications in materials science [15–18]. For these applications, resonances occurring at low projectile energies $E_p < 1$ MeV are favored, because the resolution is generally better compared to resonances at higher E_p. The signature of a nuclear resonance is the emission of reaction products in a very narrow energy window around the resonance energy E_R. Instead of detecting the energy of scattered particles, the yield curve of the resonance is obtained by varying the ion beam energy in order to excite the resonance in the surface layer and in deeper layers of the sample. The resonance yield as a function of E_p contains information of the concentration of a specific isotope as a function of depth. Comparing the yield of a narrow nuclear resonance reaction obtained from a sample to that of ion scattering, one finds a very similar situation. The energy loss processes occurring before the final collision initiates the nuclear reaction are identical. This final collision also needs the projectile to penetrate the atom at a very small impact parameter. However, as the nuclear resonance reaction leads to the formation of a compound nucleus, the projectile does not travel on an outgoing path. From the viewpoint of atomic physics this represents just one half of a scattering event. The energy resolution – and correspondingly the depth resolution – attainable by nuclear resonance experiments does not depend on the detector used for counting the reaction products. Instead the nuclear resonance can be considered as part of the ''spectrometer'', its intrinsic width Γ determines – together with other factors – the energy resolution.

As in the case of ion scattering, the yield of a nuclear resonance obtained from a sub-monolayer sample provides information on the experimental energy resolution. The FWHM of the peak located at E_R represents the experimental energy resolution consisting of contributions from the ion beam energy spread, thermal Doppler broadening and the intrinsic width Γ (Lorentzian distribution).

$$\Delta E = \frac{\Gamma}{2} + \left(\frac{\Gamma^2}{4} + \Delta E_D^2 + \Delta E_p^2 \right)^{1/2}. \quad (2)$$

And in analogy to ion scattering, the shape of the yield curve is significantly influenced by details of the single collision. Such effects become visible when measured with a system having excellent energy resolution. Different approaches have been employed to describe high-resolution resonance yields, involving a stochastic theory for energy losses as well as Monte Carlo simulations [3–6,8].

3. The signature of single collision energy loss spectra

Stopping power approaches to describe scattering spectra are based on averaging the individual energy losses to arrive at an energy loss per unit path length (or per areal density of sample atoms) [19]. As discussed above, in experiments with very high-energy resolution to detect scattered ions or measuring yield curves of narrow nuclear resonance reactions, this averaging may not be justified anymore. To describe such spectra the energy loss for individual collisions and the impact parameter dependence of the energy loss have to be considered.

A full calculation of the impact parameter dependent energy loss can be performed using first order perturbation theory which is well suited to describe ionization and excitation of sample electrons due to light ion impact [20]. Time consuming coupled-channel calculations are available for only a few selected collision systems [21,22]. Predominantly semi-empirical formula or simplified models have been used for many years to describe inelastic collisions [23–25]. Recently a simple formula for the mean electronic energy loss as a function of the impact parameter has been developed, which allows implementation in simulation codes of the slowing down of projectiles in samples [20]. Results using this approximation have been shown to be in good agreement with full first order calculations (SCA).

As an example, Fig. 1 shows the result of SCA calculations for scattering of 100 keV protons on

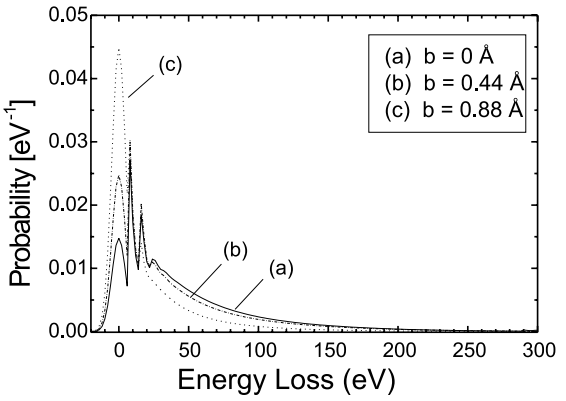

Fig. 1. Probability of energy losses as a function of the energy loss for scattering protons on carbon atoms. Spectra are shown for three different impact parameters b. The calculations are based on the SCA theory describing the collision process.

single carbon atoms at different impact parameters. It is evident that the energy loss spectrum changes significantly with the impact parameter. The average energy loss per collision with a single carbon atom varies between about 67 eV at $b = 0$ Å to about 19 eV at $b = 0.88$ Å. These numbers clearly show that a description of high-resolution spectra obtained with an energy resolution in the 10 eV range cannot be successful using simple stopping power models, especially when the samples is crystalline and certain impact parameter are favored over others. Energy losses ranging up to more than 250 eV are seen in Fig. 1. An important consequence is the following: When measuring the carbon depth distribution in steel using a backscattering geometry, a single collision 250 eV energy loss resulting from surface scattering could easily be misinterpreted as a scattering event occurring 5 Å below the sample surface.

For the case of 100 keV protons scattering on a Fe atom we found an average energy loss of about 140 eV in a zero-impact parameter collision. Assuming that the major contribution to this average energy loss is due to excitation processes in the incoming channel, the actual collision energy is reduced, leading to an increased cross section of about 0.2%. This is, however, a minor effect, especially when taking into account that significant electron screening corrections have to be applied in this projectile energy range [26–28].

Especially when using light projectiles incident on light sample nuclei, the projectile may penetrate a sample atom without suffering any energy loss due to electronic excitation. As an example, we calculated the probability for 100 keV protons penetrating through carbon atoms without suffering energy loss due to electronic excitation $P(\delta E = 0)$ using the SCA. The results show that for single sample atoms about 27% of the projectiles suffered no energy loss at an impact parameter 0. For larger impact parameters this fraction increases ($P(\delta E = 0) = 0.38$ at $b = 0.44$ Å and $P(\delta E = 0) = 0.62$ at $b = 0.88$ Å). For heavier sample atoms this probability is significantly reduced. For example we found for Cr $P(\delta E = 0) = 0.33$ at $b = 0.66$ Å and for Fe $P(\delta E = 0) = 0.08$ at $b = 0$. Even for solid samples where the probability for electronic energy losses is increased due to the neighboring atoms, a certain probability remains for no energy loss in an atomic layer. Considering very high energy-resolution measurements on ultra-thin films consisting of only a very few monolayers it is evident that the corresponding energy spectra cannot be described using a stopping power which uses a constant value energy loss per unit length.

Experimentally, single collision energy loss processes have been investigated by many authors. For example, Winter and Auth used a high-resolution electrostatic spectrometer for their studies of the energy loss of 100 keV protons in single scattering collisions with Ar atoms [29], and the impact parameter dependence of the energy loss in collisions of protons with noble gas atoms [30,31]. Using narrow nuclear resonances complementary studies have been performed at the same high-resolution accelerator facility [8,32].

To demonstrate the influence of this effect on the backscattering yield from sub-monolayer coverages of atoms on surfaces, we have measured single collision spectra of protons incident on surface sub-monolayers of sulfur and gold.

A thin layer of Au was prepared by thermal evaporation of gold on a clean Si(1 1 1) surface. Due to the subsequent annealing steps no islands are present [33]. We studied different Au coverages ranging from about 0.02 to about 0.5 monolayers. The shape of the yield curve did not change with

the coverage, indicating that indeed no islands were present. A MEIS spectrum (using 100 keV H^+-projectiles) obtained from an Au coverage of about 0.2 ML is shown in Fig. 2. The spectrum shows a distinctly asymmetric shape. The low energy tail extends several hundred eV below the peak position. SCA simulations of H^+ scattering on Au at a very small impact parameter showed that on average more than three electrons are excited in the collision making precise calculations very time consuming. Very good agreement with experimental data could therefore not be expected from the SCA algorithm. However, the large number of electron excitations leads to energy losses as large as about 1 keV in a zero impact parameter collision as shown in Fig. 2. As discussed above, an analytical approach based on stopping power data only would misinterpret the shape of the Au backscattering profile as a depth distribution extending to more than 10 Å below the surface.

For lighter elements it should be possible to describe the single collision yield in the framework of the SCA. We prepared thin sulfur surface coverages by controlled segregation of sulfur in steel, leading to a surface coverage of <0.4 ML [34]. The corresponding MEIS spectrum, again showing a significant asymmetric shape, is displayed in Fig. 3. Good agreement between experiment and theoretical results is achieved, as shown by the solid line representing the SCA calculations.

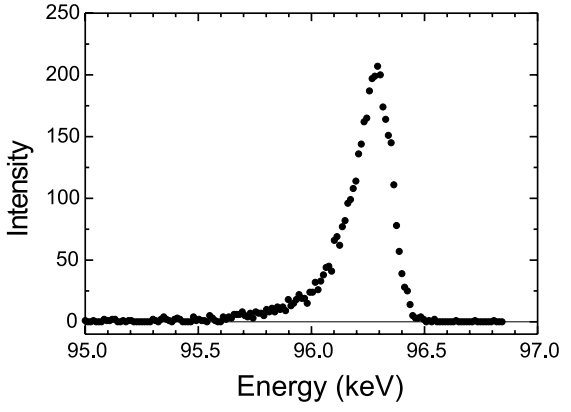

Fig. 2. Backscattering yield of 100 keV protons incident on a sub-monolayer coverage of gold.

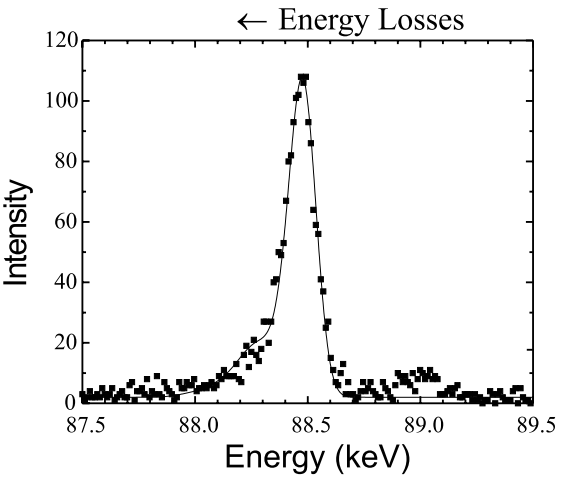

Fig. 3. Backscattering yield of 100 keV protons incident on a sub-monolayer coverage of sulfur (^{32}S). The solid line represents results of a calculation based on the SCA. The peak located at an energy of about 89 keV is due to scattering processes on other sulfur isotopes. Its intensity relative to the "^{32}S-peak" reflects the natural abundances of the isotopes ^{33}S and ^{34}S.

4. Multiple collisions

The influence of single energy loss processes is not only visible in single collision spectra, but also the shape of thick target yield curves can be influenced significantly by these processes. In the following, we will discuss one example from nuclear resonance work, which shows these effects very clearly.

Berheide et al. [7] measured the thick-target yield of the 272 keV resonance in the nuclear reaction $^{21}Ne(p,\gamma)^{22}Na$ on solid neon. This experiment was performed on an ion implantation type accelerator providing ion beam energy resolution $\Delta E_p = 10.6 \pm 1.5$ eV. Fig. 4 shows the corresponding thick target yield. The FWHM of the peak located at the resonance energy (denoted as "Lewis-Peak"), represents the experimental energy resolution, $\Delta E = 21.6$ eV (Eq. (2)), consisting of contributions from ΔE_p, ΔE_D (17.4 ± 1.6 eV, see below) and Γ (≈ 1 eV).

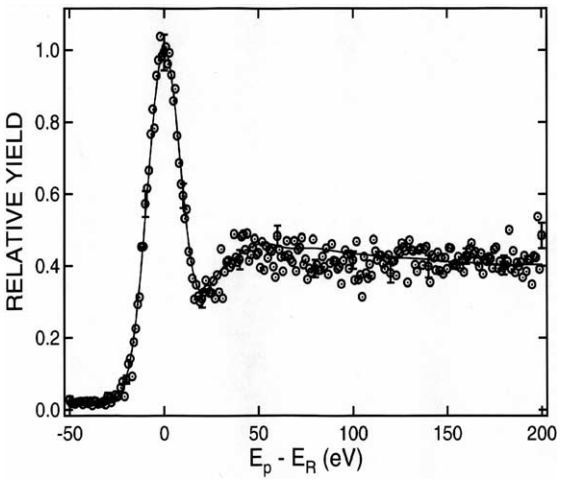

Fig. 4. Thick target yield curve of the 272 keV resonance in $^{21}Ne(p,\gamma)^{22}Na$ on solid neon. Some data points are shown with typical error bars. The solid line represents a simulation (see text for details). The experimental yield is normalized to the maximum of the fit. Energies are given relative to the resonance energy [7].

Using the stopping power cross section for 272 keV protons incident on neon atoms $\varepsilon_p = 12.2$ eV/(10^{15} atoms/cm^2) [35], the approximation for the near surface depth resolution δ is

$$\delta = \frac{\Delta E}{\varepsilon_p} = 1.8 \times 10^{15} \text{ atoms/cm}^2. \quad (3)$$

Thus a depth resolution of better than two atomic layers could be expected (1 ML $\approx 1\times 10^{15}$ atoms/cm^2, when using a Van der Waals radius of 1.54 Å [36]). Tilting the sample with respect to the ion beam axis by just 60° could easily improve this value to less than 1 ML.

However, for such a high-resolution experiment the definition of depth resolution given by Eq. (3) is not justified. Instead a detailed discussion of the energy loss processes is necessary to understand the spectrum.

- The probability for an electronic energy loss in one monolayer (P_{ML}) for the case of 272 keV protons incident on Ne-atoms is not 1 – as assumed in a continuous energy loss model. Instead it is defined by the product of the total L-shell excitation cross section (1.4×10^{-16} cm^2 [37]) and the number of atoms per monolayer: $P_{ML} \approx 14\%$. It should be noted that the contribution to the energy loss due to excitation of K-shell electrons is very small for 272 keV protons.
- The minimum electronic energy loss Q_{min} for $b \gg 0$ is defined by the minimum excitation energies of the neon atom. A value of $Q_{min} = 22 \pm 2$ eV has been found in experiments [9]. For $b \approx 0$ the electron binding energies of the compound atom (singly charged sodium) have to be considered, resulting in $Q_{min} \approx 35$ eV.
- The single collision energy loss spectrum is described by contributions due to excitation of the different L-sub-shells.
- Energy losses of more than 500 eV in a single collision have been observed.
- The measured average energy loss per collision is about (91 ± 6) eV [9]. Using this number a stopping power cross section of $\varepsilon_p = 12.9 \pm 0.9$ eV/(10^{15} atoms/cm^2) in agreement with TRIM data ($\varepsilon_p = 12.2$ eV/(10^{15} atoms/cm^2) [35]) could be calculated.

This high energy resolution spectrum (Fig. 4) does not reflect a high depth resolution. Instead the narrow peak located at the resonance energy has significant contributions from collisions (leading to the resonance reaction) as deep as 10 ML below the surface. The spectrum shows "single collision" resolution.

The solid line in Fig. 4 represents a description of the thick target yield based on a Monte Carlo simulation. In this simulation the energy loss of a single projectile is considered as the sum of discrete energy losses caused by single collisions with electrons in the neon atoms. Details of the shape of the energy loss spectra have been taken into account as well as the different shape of the energy loss process initiating the emission of the resonant γ-ray (i.e. collision at $b \approx 0$ for the incoming projectile) [7,9]. A very good description of the experimental yield curve is achieved [7].

A similar approach has to be applied for the interpretation of high-resolution ion scattering data obtained from solid samples. For the case of surface peaks obtained from crystalline samples, Alkemade et al. [14] calculated the hitting probabilities and used an impact parameter dependent

calculation of energy losses. A more detailed description of energy spectra obtained from surface peaks and ultra-thin film structures requires knowledge of energy loss spectra due to individual collision processes and includes the calculation of electronic excitation probabilities. Such calculations may be performed using the SCA as discussed above. As a result, the depth resolution of ion scattering experiments significantly depends on the sample structure and the scattering geometry.

5. Doppler broadening

An additional broadening mechanism in nuclear resonance reaction yield curves and ion scattering experiments is thermal Doppler broadening (cf. Eq. (2)). The thermal motion of sample atoms results in a Gaussian energy broadening of the yield curve of a nuclear resonance with a FWHM of ΔE_D,

$$\Delta E_D = 4\left(2\ln 2\frac{m_p}{m_S}E_R E_{kin}\right)^{1/2}, \quad (4)$$

where E_{kin} is the average kinetic energy of the sample atom due to its motion in the beam direction, and m_p and m_S are the masses of the sample atom and the projectile [7].

This effect can result in significant broadening of the resonance yield curve. It has been used to study bond strength of hydrogen atoms in the context of nuclear reaction analysis [38,39]. For the 6.4 MeV resonance in $^{15}N(p,\alpha\gamma)^{12}C, E_D$ was found to vary between 2 and 15 keV (corresponding to bond vibrational frequencies of 200–3500 cm^{-1}) depending on the chemical structure of the sample [38]. Corresponding measurements have been performed by Zinke-Allmang et al. [40], Iwata et al. [41] and Jans et al. [42]. This method has recently been extended to study hydrogen on Si(1 1 1) surfaces [43]. Special care has to be taken in these extremely sensitive experiments to obtain reliable results (see for example [44]).

For lower projectile energies and masses and heavier sample atoms, this effect contributes much less to the width of narrow resonance yield curves. However, it has been used to measure the average kinetic energy of atoms in solid neon (see above) [7].

In ion backscattering of light projectiles from heavy sample atoms Doppler broadening can be neglected in almost all practical application. For example, the energy spectrum of 100 keV protons backscattered from gold is widened by an additional Gaussian contribution of approximately 10 eV. However, when using heavier projectiles this effect may no longer be neglected. It may even offer the potential to study the kinetic energy of surface and near-surface atoms.

For ERD experiments, the influence of thermal Doppler broadening has been discussed by Lanford [38]. As an example, 1.7 MeV ^{4}He incident on hydrogen would result in a Doppler broadening of about 1 keV. This is a small contribution, but as mentioned by Lanford, it should be measurable.

Copel and Tromp measured hydrogen on HF-etched Si(0 0 1) using MEIS in an ERD configuration by applying a time-of-flight technique to discriminate recoil hydrogen ions from scattered projectiles [45]. In their experiment, they used 220 keV ^{7}Li projectiles and obtained a depth resolution of about 9 Å corresponding to a peak width of about 700 eV. For this projectile – sample atom configuration a Doppler broadening varying from less than 100 eV to about 500 eV could be expected depending on the chemical bond strength. Using a thermal energy of 0.13 eV for the hydrogen bond on Si(0 0 1), the resulting Doppler broadening could be as large as 300 eV in their configuration. This is a major contribution to the energy resolution of the system and clearly a limitation of the achievable depth resolution.

6. Summary

High-resolution depth profiling experiments are important analytical tools to help understand the characteristics of surfaces and thin films and to facilitate their technological applications. Recently, a number of ion scattering facilities have been designed in order to achieve monolayer depth resolution. Such high-resolution spectra,

however, cannot always be precisely described using approaches such as stopping power and straggling formalisms. To illustrate related problems, we have performed theoretical and experimental studies. To understand the shape of high-energy resolution ion backscattering spectra SCA calculations have been performed, describing the impact parameter dependent energy loss in single ion–atom collisions. Experiments were performed using a MEIS system. Good agreement was found between theoretical description and experimental data for the case of scattered protons from a sub-monolayer coverage of sulfur atoms. The results show that the impact parameter dependent energy loss in a single ion atom collision can significantly influence the interpretation of experimental results. The influence of thermal vibrations of the sample atoms on the backscattering spectra has been discussed. The significance of Doppler broadening in ion scattering yields obtained from high-resolution experiments may be utilized for future studies of thermal vibrations.

Acknowledgements

This work was supported in part by the NSF through grants DMR-9701748 and EEC-9720424.

References

[1] G.G. Ross, B. Terreault, Nucl. Instr. and Meth. B 15 (1986) 146.
[2] H.W. Lewis, Phys. Rev. 125 (1962) 937.
[3] W.L. Walters, D.G. Costello, J.G. Skofronick, D.W. Palmers, W.E. Kane, R.G. Herb, Phys. Rev. 125 (1962) 2012.
[4] B. Maurel, G. Amsel, J.P. Nadai, Nucl. Instr. and Meth. 197 (1982) 1.
[5] I. Vickridge, G. Amsel, Nucl. Instr. and Meth. B 45 (1990) 6.
[6] I. Vickridge, G. Amsel, Nucl. Instr. and Meth. B 85 (1994) 566.
[7] M. Berheide, W.H. Schulte, H.W. Becker, L. Borucki, M. Buschmann, C. Rolfs, Phys. Rev. B 58 (1998) 11103.
[8] W.H. Schulte, H. Ebbing, S. Wüstenbecker, H.W. Becker, M. Berheide, M. Buschmann, C. Rolfs, G.E. Mitchell, J.S. Schweitzer, Nucl. Instr. and Meth. B 71 (1992) 291.
[9] W.H. Schulte, H. Ebbing, H.W. Becker, M. Berheide, M. Buschmann, C. Rolfs, G.E. Mitchell, J.S. Schweitzer, J. Phys. B 27 (1994) 5271.
[10] S. Deckers, F.H.P.M. Habraken, W.F. van der Veg, A.W. Denier van der Gon, B. Bluis, J.F. van der Veen, R. Baudoing, Phys. Rev. B 40 (1990) 3253.
[11] B.W. Busch, W.H. Schulte, T. Gustafsson, C. Uebing, Nucl. Instr. and Meth. B 183 (2001) 88.
[12] J.W.M. Frenken, R.M. Tromp, W.F. van der Veen, Nucl. Instr. and Meth. B 17 (1986) 334.
[13] P.F.A. Alkemade, W.C. Turkenburg, J. Vrijmoeth, Nucl. Instr. and Meth. B 64 (1992) 716.
[14] P.F.A. Alkemade, W.C. Turkenburg, W.F. van der Weg, Nucl. Instr. and Meth. B 28 (1987) 161.
[15] G. Battistig, G. Amsel, E. d'Artemare, I. Vickridge, Nucl. Instr. and Meth. B 61 (1991) 369.
[16] G. Battistig, G. Amsel, E. d'Artemare, I. Vickridge, Nucl. Instr. and Meth. B 66 (1992) 1.
[17] T. Åkermark, L.G. Gosset, J.-J. Ganem, I. Trimaille, I. Vickridge, S. Rigo, J. Appl. Phys. 86 (1999) 1153.
[18] I.J.R. Baumvol, C. Krug, F.C. Stedile, F. Gorris, W.H. Schulte, Phys. Rev. B 60 (1999) 1492.
[19] J.F. Ziegler, Nucl. Instr. and Meth. 168 (1980) 17.
[20] P.L. Grande, G. Schiwietz, Phys. Rev. A 58 (1998) 3796.
[21] G. Schiwietz, Phys. Rev. A 42 (1990) 296.
[22] P.L. Grande, G. Schiwietz, Nucl. Instr. and Meth. B 132 (1997) 264.
[23] O. Oen, M. Robinson, Nucl. Instr. and Meth. 132 (1976) 647.
[24] O.B. Firsov, Sov. Phys. JETG 9 (1959) 1076.
[25] J. Lindhard, A. Winther, K. Dan. Vidensk. Selsk. Mat. Fys. Medd. 34 (1964) 4.
[26] H.H. Anderson, F. Besenbacher, P. Loftager, W. Möller, Phys. Rev. A 21 (1980) 1891.
[27] E. Huttel, W. Arnold, J. Baumgart, G. Clausnitzer, Nucl. Instr. and Meth. B 12 (1985) 193.
[28] S.R. Lee, R.R. Hart, Nucl. Instr. and Meth. B 79 (1993) 463.
[29] C. Auth, H. Winter, Nucl. Instr. and Meth. A 176 (1993) 109.
[30] C. Auth, H. Winter, Nucl. Instr. and Meth. B 93 (1994) 123.
[31] G. Schiwietz, P.L. Grande, C. Auth, H. Winter, A. Salin, Phys. Rev. Lett. 72 (1994) 2159.
[32] W.H. Schulte, Thesis, Universität Münster, Germany, 1989.
[33] M. Chester, T. Gustafsson, Surf. Sci. 256 (1991) 135.
[34] B.W. Busch, T. Gustafsson, C. Uebing, APL 74 (1999) 3564.
[35] J.F. Ziegler, J.P. Biersack, SRIM-2000 (v.09), IBM-Research, Yorktown, NY.
[36] A. Bondi, J. Phys. Chem. 68 (1964) 441.
[37] J.B. Crooks, M.E. Rudd, Phys. Rev. A 3 (1971) 1628.
[38] W.A. Lanford, Nucl. Instr. and Meth. B 66 (1992) 65.
[39] L. Borucki, H.W. Becker, F. Gorris, S. Kubsky, W.H. Schulte, C. Rolfs, Eur. Phys. J. A 5 (1999) 327.
[40] M. Zinke-Allmang, S. Kalbitzer, M. Weiser, Z. Phys. A (1986) 183.

[41] Y. Iwata, F. Fujimoto, E. Vilalta, A. Ootuka, K. Komaki, H. Yamashita, Y. Murata, Nucl. Instr. and Meth. B 33 (1988) 574.
[42] S. Jans, S. Kalbitzer, P. Oberschachtsiek, J.P.F. Sellschop, Nucl. Instr. and Meth. B 85 (1994) 321.
[43] B. Hartmann, S. Kalbitzer, M. Behar, Nucl. Instr. and Meth. B 103 (1995) 494.
[44] K.H. Ecker, J. Krauser, A. Weidinger, H.P. Weise, K. Maser, Nucl. Instr. and Meth. B 161–163 (2000) 682.
[45] M. Copel, R.M. Tromp, Rev. Sci. Instr. 64 (1993) 3147.